INTERNATIONAL JOURNAL OF MECHANICS
DOI: 10.46300/9104.2022.16.7 Volume 16, 2022

A three-dimensional multi-species flow solver for the Euler equations combined with a stiffened gas equation of state

Hind Benakrach, Mohamed Bounouib, Mourad Taha-Janan, Mohamed Zeriab Essadek
Laboratory of Applied Mechanics and Technologies (LaMAT),
Ensam, B.P., 6207 Av. des Forces Armées Royales, Rabat ,10100
Morocco

Received: April 10, 2021. Revised: March 15, 2022. Accepted: April 12, 2022. Published: May 17, 2022.

Abstract- Although numerical simulation in fluid mechanics is undergoing a significant development due to the dazzling evolution of computing means, complex physical phenomena, such as multidimensional viscous effects in turbomachinery and cavitation, remain mysterious and attract the curiosity of several researchers. High-resolution shock captures are often obtained by the WENO family of schemes, except that in problems that depend on discontinuities and shocks, an appearance of numerical oscillations weakens its ability to provide adequate captures. The use of the characteristic construction methods prevents this type of oscillation. The present paper contributes to the numerical resolution of multi-species flows of viscous, compressible, or incompressible fluids with shocks and discontinuities. The proposed numerical model can handle various configurations with a unique method based on a conservative and consistent three-dimensional finite volume scheme with an aligned mesh. The system of equations is a set of Euler equations coupled with a two-parameters generalized state equation of state in three-dimensional Cartesian coordinates. This system is solved using a Roe type approximate Riemann solver, and second-order precision is obtained using limiters. The obtained numerical results maintain a non-oscillatory flow near the discontinuities, which makes the method satisfactory and shows its accuracy and robustness in different cases.

Keywords- Euler's equation, Finite volume method, Roe solver, Multi-component flows, shock tube, Richtmyer–Meshkov instability.

I. Introduction

DIFFERENT numerical methods can simulate the flows with discontinuities. However, to get an accurate and high-resolution simulation, these numerical methods must capture all the essential characteristics by rigorously selecting the equation that correctly describes this type of flow. The choice of how to differentiate convective terms is crucial for treating fluid flows. In this context, the finite volume method is chosen from many well-known numerical methods. It is commonly used in fluid mechanics thanks to its inherent property of preserving the flows of the quantities transported. Toro [1] and LeVeque [2] are good references for understanding these methods.

To solve hyperbolic equations, Godunov [3] presented a numerical method capable of taking into account discontinuities. The method is based on an explicit decentralized scheme by proposing to compute the flows allowing the evolution of the variables by considering a series of local Riemann problems. The solution of non-linear systems of equations requires a generalized Riemann problem [4]. To support quasi-linear approaches, some researchers have devoted efforts to improving the process of calculating flows by improving the Godunov 'scheme. Although it is very efficient for capturing shocks, Godunov's method is a first-order method. Therefore several authors have proposed extensions to build higher-order schemes [5, 6, 7] .

Among Riemann's various approximate problem solvers, and despite criticism by some authors, especially Quirk [8], Roe's scheme remains one of the most popular ones known for its effectiveness in treating flows with discontinuities. From its appearance in 1981, the Roe scheme could not calculate rarefaction shock waves. The Roe type approximate solver is extended to a higher order in space by so-called high-resolution schemes that manage dissipation, if necessary, to eliminate non-physical oscillations.

Higher-order spatial accuracy could be achieved by using more accurate schemes such as the Monotonic Upstream-Centered Scheme for Conservation Laws (MUSCL) technique [9, 10]. This technique is performed by interpolation followed by limiting to minimize numerical oscillations near discontinuity regions. The numerical flow expression introduces flow extrapolation belonging to the family of total decreasing variation (TDV)

schemes and slope limiting methods [11]. The different limiters encourage them to choose the most appropriate one[12]. Other methods are not part of the TVD family but respect the property of being non-oscillatory like the ENO (Essentially Not Oscillating) schemes initiated by Harten [11, 12, 13], , or the ADER (Arbitrary accuracy DErivates Riemann problem) of Toro[14, 15]. A comparison between these reconstruction techniques was the subject of Deng's paper [16].

Regarding a formulation that considers the presence of more than one fluid, it was chosen so that the model will allow the simulation of a wide range of situations. Therefore, the model is based on a stiffened equation of state characterized by two parameters, allowing each species to be determined. This equation has shown its effectiveness in work carried out by Shyue [17].

Taha-Janan and El Marjani [18] studied multi-species flows in curvilinear coordinates. The finite difference method solved a combination of the two-dimensional Navier-Stokes and Euler equations with the gamma model. Roe's flow-difference splitting approach was adopted for better accuracy. The present work extends for three-dimensional flow cases using the Cartesian coordinate system. Validation by single and multi-species flows has been performed, the results obtained are close to the results presented in the literature.

II. MATHEMATICAL FORMULATION

The three-dimensional flow of a non-viscous fluid is described by the Euler in a Cartesian coordinate system, the system can be written in the following conservative form:

$$\frac{\partial}{\partial t}\begin{pmatrix}\rho\\ \rho u\\ \rho v\\ \rho w\\ \rho E_0\end{pmatrix}+\frac{\partial}{\partial x}\begin{pmatrix}\rho u\\ \rho u^2+p\\ \rho uv\\ \rho uw\\ (\rho E_0+p)u\end{pmatrix}+\frac{\partial}{\partial y}\begin{pmatrix}\rho v\\ \rho uv\\ \rho v^2+p\\ \rho vw\\ (\rho E_0+p)v\end{pmatrix}+\frac{\partial}{\partial z}\begin{pmatrix}\rho w\\ \rho uw\\ \rho vw\\ \rho w^2+p\\ (\rho E_0+p)w\end{pmatrix}=0$$

Where the density ρ of the fluid is assumed to be variable. u, v and w are the components of the velocity vector in the considered Cartesian reference,p is static pressure and E_0 is the total mass energy expressed as:

$$E_0 = e + \frac{1}{2}\left(u^2+v^2+w^2\right) \tag{1}$$

With e representing the internal energy mass of the fluid. This system requires, for its closure, the use of a thermodynamic equation which is the two-parameter stiffened gas equation of state. This equation is often presented in the study of multi-component compressible flows [19, 20, 21].The internal energy and pressure of the gas or liquid is related by the equation :

$$\rho e = \frac{p+\gamma p_\infty}{\gamma-1} \tag{2}$$

γ is the usual ratio of specific heats and p_∞ is a prescribed pressure constant. These parameters are determined from laboratory experiments via empirical adjustment. The associated speed of sound is given by :

$$a = \sqrt{(\gamma-1)\left(H-\frac{1}{2}(u^2+v^2+w^2)\right)} \tag{3}$$

The pressure is written as follows:

$$p = (\gamma-1)\left(E_0-\frac{1}{2}\rho(u^2+v^2+w^2)\right) \tag{4}$$

Equations for the two parameters appearing in the stiffened gas equation can be obtained considering the case of an interface-only problem where pressure and speed are constant in the domain, while the other variables (ρ,γ,p_∞) have jumps across some interface. Based on these conditions and using the non-conservative formula of the Euler equations, the energy equation combined with the state equation makes it easy to obtain:

$$\frac{\partial}{\partial t}\left(\frac{p+\gamma p_\infty}{+a-1}\right)+u\frac{\partial}{\partial x}\left(\frac{p+\gamma p_\infty}{\gamma-1}\right)+v\frac{\partial}{\partial y}\left(\frac{p+\gamma p_\infty}{\gamma-1}\right)+w\frac{\partial}{\partial z}\left(\frac{p+\gamma p_\infty}{\gamma-1}\right)=0$$

The imposed condition on the pressure, whether regarding the equilibrium or its applicability everywhere in the physical space, makes it possible to obtain a system of two equations that must be satisfied for the variables γ and p_∞. These equations are as follows:

$$\begin{cases}\dfrac{\partial}{\partial t}\left(\dfrac{1}{\gamma-1}\right)+u\dfrac{\partial}{\partial x}\left(\dfrac{1}{\gamma-1}\right)+v\dfrac{\partial}{\partial y}\left(\dfrac{1}{\gamma-1}\right)+w\dfrac{\partial}{\partial z}\left(\dfrac{1}{\gamma-1}\right)=0\\ \dfrac{\partial}{\partial t}\left(\dfrac{\gamma p_\infty}{\gamma-1}\right)+u\dfrac{\partial}{\partial x}\left(\dfrac{\gamma p_\infty}{\gamma-1}\right)+v\dfrac{\partial}{\partial y}\left(\dfrac{\gamma p_\infty}{\gamma-1}\right)+w\dfrac{\partial}{\partial z}\left(\dfrac{\gamma p_\infty}{\gamma-1}\right)=0\end{cases}$$

Adding these two equations to Euler's system of equations, the complete system is obtained, which allows to solve multi-component problems with the state equation of the stiffened gas, described above:

$$\frac{\partial q}{\partial t}+\frac{\partial E}{\partial x}+\frac{\partial F}{\partial y}+\frac{\partial G}{\partial z}=0 \tag{5}$$

With :

$$q = \begin{pmatrix} \rho \\ \rho u \\ \rho v \\ \rho w \\ \rho E_0 \\ \frac{\rho}{\gamma-1} \\ \frac{\rho\gamma p_\infty}{\gamma-1} \end{pmatrix}; E = \begin{pmatrix} \rho u \\ \rho u^2 + p \\ \rho uv \\ \rho uw \\ (\rho E_0 + p)u \\ \frac{\rho u}{\gamma-1} \\ \frac{\rho u\gamma p_\infty}{\gamma-1} \end{pmatrix};$$

$$F = \begin{pmatrix} \rho v \\ \rho uv \\ \rho v^2 + p \\ \rho vw \\ (\rho E_0 + p)v \\ \frac{\rho v}{\gamma-1} \\ \frac{\rho v\gamma p_\infty}{\gamma-1} \end{pmatrix}; G = \begin{pmatrix} \rho w \\ \rho uw \\ \rho vw \\ \rho w^2 + p \\ (\rho E_0 + p)w \\ \frac{\rho w}{\gamma-1} \\ \frac{\rho w\gamma p_\infty}{\gamma-1} \end{pmatrix}$$

The previous system can also be presented in a non-conservative form, showing the Jacobian matrices $A(q)$, $B(q)$ and $C(q)$ of the flow:

$$\frac{\partial q}{\partial t} + A(q)\frac{\partial q}{\partial x} + B(q)\frac{\partial q}{\partial y} + C(q)\frac{\partial q}{\partial z} = 0 \qquad (6)$$

With:

$$A(q) = \frac{\partial E}{\partial q}; B(q) = \frac{\partial F}{\partial q}; C(q) = \frac{\partial G}{\partial q};$$

One of the strengths of this method is its ability to calculate the distribution of species present in the flow using only always seven equations regardless of the number of species for the three-dimensional case.

In order to reproduce the behaviors of the fluids, the direct resolution of this system of equations proves to be very complex. It is therefore necessary to use numerical solving methods in order to easily generate new configurations and to better understand the problem and predict its physics.

III. NUMERICAL APPROXIMATION OF THE SYSTEM

The objective of the present work is to develop a simple and precise numerical method on a Cartesian coordinates system. This section mainly contains the methods as well as the numerical approximations used for the construction of the calculation code. In order to simplify the presentation of the model, the numerical scheme is expressed for a one-dimensional system.

The problem studied in this article is solved using the high resolution wave propagation method. This requires a general presentation of the Godunov method, method of Roe, as well as integration of the limiter to switch spatial precision order to another.

A. NUMERICAL METHOD

Discretization is done by finite volume methods, which is a method that has a great interest to be intrinsically conservative and fits perfectly to the discontinuous aspect of the problem. Godunov [3] suggested to solve Riemann's problem at each time step by keeping all the conservative variables constant on each mesh, this temporal evolution is obtained by the exact resolution of the problem. The method is thus presented in the following conservative form:

$$q_i^{n+1} =^n -\frac{\Delta t}{\Delta x}\left[E^*_{i+\frac{1}{2}} - E^*_{i-\frac{1}{2}}\right] - \frac{\Delta t}{\Delta y}\left[F^*_{j+\frac{1}{2}} - F^*_{j-\frac{1}{2}}\right] - \frac{\Delta t}{\Delta z}\left[G^*_{k+\frac{1}{2}} - G^*_{k-\frac{1}{2}}\right]$$

Where The numerical flux $E_{i\pm\frac{1}{2}}$, $F_{i\pm\frac{1}{2}}$ and $G_{i\pm\frac{1}{2}}$ are calculated from the exact solution.

Although Godunov's method allows to compute numerical flows based on the exact solution of Riemann's problem, it proves to be expensive in terms of computation time. Calculating the exact solution on average over each grid cell introduces numerical errors. To mitigate this, it is therefore necessary to use other methods which will be based on certain approximations. These methods are often known as Riemann solvers or Riemann schemes, their role is to calculate the flows at the interfaces by less expensive means of calculation. Some relevant approximate Riemann solvers are presented in Toro's work [22].

Roe [6] has developed an important class of Riemann Solvers which has formed the basis of the schemes used in many current methods. His approach allows to linearize the system by changing the Jacobian matrix by a matrix, called a Roe matrix. For a first-order decentralization using first order Roe decomposition (using first order Roe flux differencing [6, 23, 24, 25], the numerical flows of the convective vectors $\overline{E}$, $\overline{F}$, $\overline{G}$ are written as :

$$\begin{cases} E^*_{i+\frac{1}{2}} = \frac{1}{2}(\overline{E}_i + \overline{E}_{i+1}) + D_{i+\frac{1}{2}} \\ F^*_{j+\frac{1}{2}} = \frac{1}{2}(\overline{F}_j + \overline{F}_{j+1}) + D_{j+\frac{1}{2}} \\ G^*_{k+\frac{1}{2}} = \frac{1}{2}(\overline{G}_k + \overline{G}_{k+1}) + D_{k+\frac{1}{2}} \end{cases} \qquad (7)$$

$D_{i+\frac{1}{2}}$, $D_{j+\frac{1}{2}}$ and $D_{k+\frac{1}{2}}$ are the terms which determine the type and the order of precision of the discretization. For the first order, they are given by:

$$\begin{cases} D^{(1)}_{i+\frac{1}{2}} = -\frac{1}{2}\left|\tilde{A}_{i+\frac{1}{2}}\right|(q_{i+1} - q_i) \\ D^{(1)}_{j+\frac{1}{2}} = -\frac{1}{2}\left|\tilde{B}_{j+\frac{1}{2}}\right|(q_{j+1} - q_j) \\ D^{(1)}_{k+\frac{1}{2}} = -\frac{1}{2}\left|\tilde{C}_{k+\frac{1}{2}}\right|(q_{k+1} - q_k) \end{cases}$$

$\tilde{A}_{i+\frac{1}{2}}$, $\tilde{B}_{j+\frac{1}{2}}$ and $\tilde{C}_{k+\frac{1}{2}}$ are called Roe's matrices. In Cartesian coordinates, their expressions are expressed by:

$$D_{k+\frac{1}{2}}^{(2,3)} = -\frac{1}{2}\left|\tilde{C}_{k+\frac{1}{2}}\right|(q_{k+1}-q_k) + \frac{1}{4}\Big\{(1-\kappa)\Psi_{k-\frac{1}{2}}^{+}\tilde{C}_{k-\frac{1}{2}}^{+}(q_k-q_{k-1}) + (1+\kappa)\Psi_{k+\frac{1}{2}}^{-}\tilde{C}_{k+\frac{1}{2}}^{+}(q_{k+1}-q_k)$$
$$-(1-\kappa)\Psi_{k-\frac{1}{2}}^{+}\tilde{C}_{k+\frac{1}{2}}^{-}(q_{k+1}-q_k) - (1-\kappa)\Psi_{k+\frac{3}{2}}^{-}\tilde{C}_{k+\frac{3}{2}}^{-}(q_{k+2}-q_{k+1})\Big\}$$

$$\tilde{A} = \begin{pmatrix} 0 & 1 & 0 & 0 & 0 & 0 & 0 \\ \left(\frac{\gamma-3}{2}\right)\overline{u}^2 + \left(\frac{\gamma-1}{2}\right)(\overline{v}^2+\overline{w}^2) & (3-\gamma)\overline{u} & (1-\gamma)\overline{v} & (1-\gamma)\overline{w} & \gamma-1 & \overline{\chi} & 1-\gamma \\ -\overline{uv} & \overline{v} & \overline{u} & 0 & 0 & 0 & 0 \\ -\overline{uw} & \overline{w} & 0 & \overline{u} & 0 & 0 & 0 \\ \left(\frac{\gamma-1}{2}\right)\overline{u}(\overline{u}^2+\overline{v}^2+\overline{w}^2) - \overline{u}\overline{H} & (1-\gamma)\overline{u}^2 + \overline{H} & (1-\gamma)\overline{uv} & (1-\gamma)\overline{uw} & \gamma\overline{u} & \overline{\chi u} & (1-\gamma)\overline{u} \\ 0 & 0 & 0 & 0 & 0 & \overline{u} & 0 \\ 0 & 0 & 0 & 0 & 0 & 0 & \overline{u} \end{pmatrix}$$

$$\tilde{B} = \begin{pmatrix} 0 & 0 & 1 & 0 & 0 & 0 & 0 \\ -\overline{uv} & \overline{v} & \overline{u} & 0 & 0 & 0 & 0 \\ \left(\frac{\gamma-3}{2}\right)\overline{v}^2 + \left(\frac{\gamma-1}{2}\right)(\overline{u}^2+\overline{w}^2) & (1-\gamma)\overline{u} & (3-\gamma)\overline{v} & (1-\gamma)\overline{w} & \gamma-1 & \overline{\chi} & 1-\gamma \\ -\overline{vw} & 0 & \overline{w} & \overline{v} & 0 & 0 & 0 \\ \left(\frac{\gamma-1}{2}\right)\overline{v}(\overline{u}^2+\overline{v}^2+\overline{w}^2) - \overline{v}\overline{H} & (1-\gamma)\overline{uv} & (1-\gamma)\overline{v}^2 + \overline{H} & (1-\gamma)\overline{vw} & \gamma\overline{v} & \overline{\chi v} & (1-\gamma)\overline{v} \\ 0 & 0 & 0 & 0 & 0 & \overline{v} & 0 \\ 0 & 0 & 0 & 0 & 0 & 0 & \overline{v} \end{pmatrix}$$

$$\tilde{C} = \begin{pmatrix} 0 & 0 & 0 & 1 & 0 & 0 & 0 \\ -\overline{uw} & \overline{w} & 0 & \overline{u} & 0 & 0 & 0 \\ -\overline{vw} & 0 & \overline{w} & \overline{v} & 0 & 0 & 0 \\ \left(\frac{\gamma-3}{2}\right)\overline{w}^2 + \left(\frac{\gamma-1}{2}\right)(\overline{u}^2+\overline{v}^2) & (1-\gamma)\overline{u} & (1-\gamma)\overline{v} & (3-\gamma)\overline{w} & \gamma-1 & \overline{\chi} & 1-\gamma \\ \left(\frac{\gamma-1}{2}\right)\overline{w}(\overline{u}^2+\overline{v}^2+\overline{w}^2) - \overline{w}\overline{H} & (1-\gamma)\overline{uw} & (1-\gamma)\overline{vw} & (1-\gamma)\overline{w}^2 + \overline{H} & \gamma\overline{w} & \overline{\chi w} & (1-\gamma)\overline{w} \\ 0 & 0 & 0 & 0 & 0 & \overline{w} & 0 \\ 0 & 0 & 0 & 0 & 0 & 0 & \overline{w} \end{pmatrix}$$

B. FLUX LIMITERS

In practice, a resolution obtained by first-order spatial accuracy prevents the obtaining of acute shocks. So-called high-resolution methods are used to fill these gaps. A wide range of Total Variation Diminishing (TVD) schemes, combined with a limitation procedure, helps avoid unnecessary fluctuations near discontinuities [14]. Three types of limiters will be used in this work: Van Leer limiter, Van Albada limiter and Superbee limiter.

For up to third-order accuracy [18], the flow is written as follows:

$$D_{i+\frac{1}{2}}^{(2,3)} = -\frac{1}{2}\left|\tilde{A}_{i+\frac{1}{2}}\right|(q_{i+1}-q_i) + \frac{1}{4}\Big\{(1-\kappa)\Psi_{i-\frac{1}{2}}^{+}\tilde{A}_{i-\frac{1}{2}}^{+}(q_i-q_{i-1}) + (1+\kappa)\Psi_{i+\frac{1}{2}}^{-}\tilde{A}_{i+\frac{1}{2}}^{+}(q_{i+1}-q_i)$$
$$-(1-\kappa)\Psi_{i-\frac{1}{2}}^{+}\tilde{A}_{i+\frac{1}{2}}^{-}(q_{i+1}-q_i) - (1-\kappa)\Psi_{i+\frac{3}{2}}^{-}\tilde{A}_{i+\frac{3}{2}}^{-}(q_{i+2}-q_{i+1})\Big\}$$

$$D_{j+\frac{1}{2}}^{(2,3)} = -\frac{1}{2}\left|\tilde{B}_{j+\frac{1}{2}}\right|(q_{j+1}-q_j) + \frac{1}{4}\Big\{(1-\kappa)\Psi_{j-\frac{1}{2}}^{+}\tilde{B}_{j-\frac{1}{2}}^{+}(q_j-q_{j-1}) + (1+\kappa)\Psi_{j+\frac{1}{2}}^{-}\tilde{B}_{j+\frac{1}{2}}^{+}(q_{j+1}-q_j)$$
$$-(1-\kappa)\Psi_{j-\frac{1}{2}}^{+}\tilde{B}_{j+\frac{1}{2}}^{-}(q_{j+1}-q_j) - (1-\kappa)\Psi_{j+\frac{3}{2}}^{-}\tilde{B}_{j+\frac{3}{2}}^{-}(q_{j+2}-q_{j+1})\Big\} \quad (8)$$

The parameter Ψ is equal to the unit for smooth solutions and has the expression of a limiter in the presence of shocks or contact discontinuities. Whereas κ allows the order to be adjusted. It is second order if $\kappa = -1$ and up to third order if $\kappa = 1/3$.

IV. NUMERICAL TESTS

A. INTRODUCTION

The proposed method promises its capability of solving numerically, in the presence of shock, single-specie or multi-species flows. A previous work [26] carried out for a single-species flow allowed us to favor a second order precision with the use of limiters, which smooths the solution at discontinuities. The ultimate goal of a limiter is to suppress the oscillations that appear when using a second order spatial precision, so it has shown the validity of the Cartesian aligned mesh in one and two dimensions. The illustration of the main characteristics of the algorithm proposed in this work is made from the various numerical tests proposed in this section. Several numerical simulations have been performed to evaluate the ability of the solver to reproduce and handle well identified numerical problems.

The first step is to test its performance by comparing the results obtained and the exact solutions from the literature. Since the model described here is based on the two-parameter general state equation that ensures the transition from single-species to multi-species flow without any difficulty, a second step will consist of testing on multi-species flows.

A validation of the 3D model is performed for the different dimensions. For this, the initial conditions and boundary conditions are taken so that the flow is compatible with the dimension of the reference model. All calculations were performed on a single processor computer.

B. VALIDATION OF THE MODEL

B..1 Single-specie flow

For the first validation test, an analytical solution of the Sod shock tube problem was used for the validation of the 1D model where the fluid moves only along the x-axis. This problem is considered as one of the most standard numerical references used for the validation of solvers dealing with compressible flows [27, 28], it consists in solving the one-dimensional Euler equations for a compressible fluid in which a rarefaction wave, a contact discontinuity and a shock discontinuity propagate.

In this problem, two fluids placed in a tube and separated initially in the middle by an ideal diaphragm, these two fluids in both sections are initially at rest. The state of the fluid on the left is characterized by $(\rho, u, v, w, p, \gamma, p_\infty)_L = (1.0, 0.0, 0.0, 0.0, 1.0, 1.4, 0.0)_L$. For up to third-order accuracy and the fluid in the right half of the tube is characterized by $(\rho, u, v, w, p, \gamma, p_\infty)_R = (0.125, 0.0, 0.0, 0.0, 0.1, 1.4, 0.0)_R$. The flow is along the x-axis and the domain is discretized by $[400 \times 2 \times 2]$ grid points and the time step is set at $\Delta t = 10^{-4} s$.

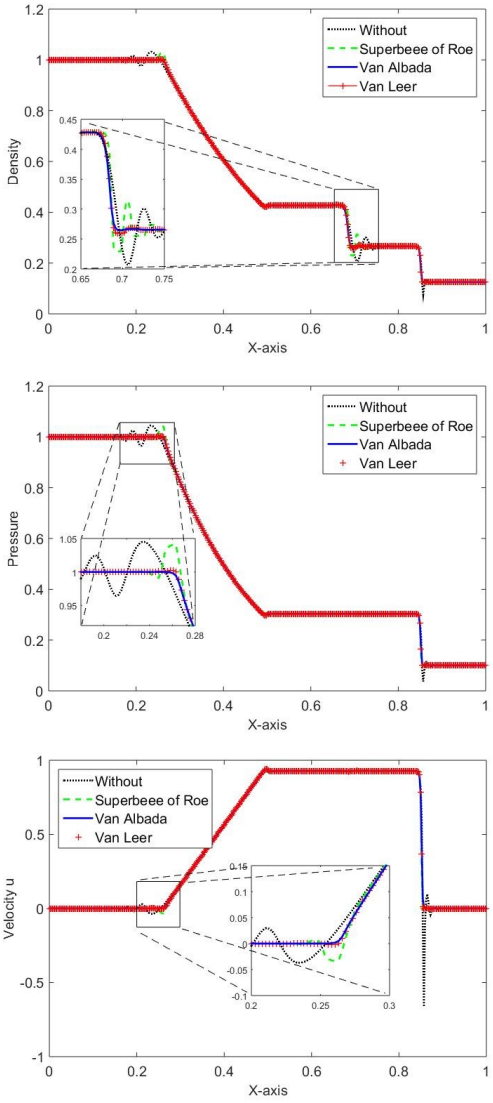

Fig. 1: Comparison of solutions with and without limiter for the profiles of density, pressure and velocity obtained along the x-axis.

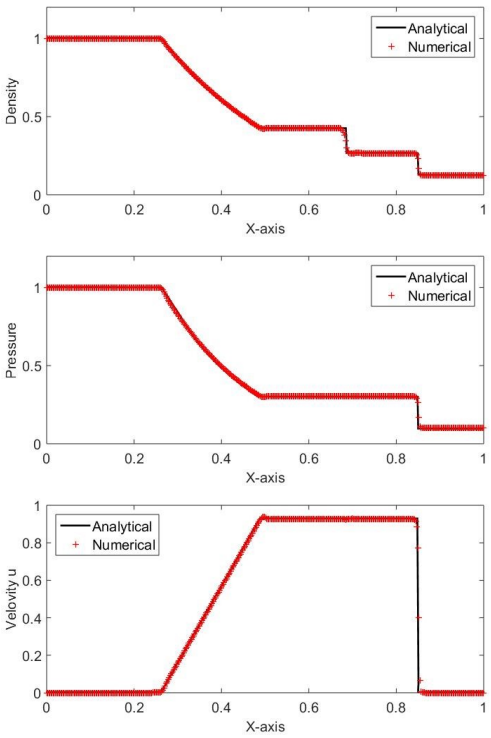

Fig. 2: Comparison of analytical and numerical results using Van Leer limiter for density, pressure and velocity profiles.

The comparison between the analytical solution and the numerical results of the adopted model at $t_{final} = 0.2s$ is presented in Figures 1 and 2, it groups together the profiles of the evolution of the pressure, the velocity and the fluids density along the tube.

It can be seen that a 2nd order precision with the Van Leer or Van Albada limiters allows to obtain a solution profile without oscillations with a high resolution around the contact discontinuity and shock (Fig. 1). It is clear that the solution using such limiters with a second-order precision compare very good with the reference solution (Fig. 2). The proposed algorithm is therefore capable of adequately capturing the shocks presented in mono-species flows.

B..2 Multi-specie flow

Let's consider an interface that separates a gas at high pressure and a liquid at low pressure [17, 29, 30]. The initial state is defined as follows:

$$\begin{cases} (\rho, u, v, w, p, \gamma, p_\infty)_L = (1.241, 0.0, 0.0, 0.0, 2.753, 1.4, 0.0), & 0x < 0.5 \\ (\rho, u, v, w, p, \gamma, p_\infty)_L = (0.991, 0.0, 0.0, 0.0, 3.059 \times 10^{-4}, 5.4, 1.505), & 0.5x < 1 \end{cases}$$

The computations are carried out using a Courant-Friedrich-Lewy number (CFL) of 0.5 is chosen to keep the numerical stability, the domain contains $[400 \times 2 \times 2]$ meshes, the idea is to realize a flow following x which allows the comparison of the analytical results at 1D and the results obtained at 3D. The Van Albada limiter is used.

Figure 3 shows the different profiles of density, pressure, velocity, p_∞ parameter and heat capacity ratio γ obtained at $t = 0.1s$, using the code in comparison with the analytical results.

The profiles presented in figure 3 allow the validation of the models chosen in this work, the algorithm allows to capture exactly the contact discontinuity without excessive numerical dissipation.

C. 2D SHOCK TUBE PROBLEM

A 2D Sod shock is performed in the proposed model on a cylinder with base radius $r = 1/6$ centered in a cube $[0, 1] \times [0, 1] \times [0, 1]$. The cylinder is filled with a gas of density $\rho_c = 1$, velocity $u_c = v_c = w_c = 0$, a pressure $p_c = 1$ and $\gamma_c = 1.4$, while the rest of the domain is initiated by: $(\rho, u, v, w, p, \gamma, p_\infty)_{cube} = (0, 125, 0, 0, 0, 0.1, 1.6, 0)$. The calculation was carried out with $[200 \times 200 \times 2]$ meshes.

Figure. 4 represents the evolution of density, velocity u, pressure, parameter p_∞ and heat capacity ratio along the x-axis at $t_{final} = 0.025$, y and z were set at 0.5. While Figure 5 shows the density and pressure distribution in the (xy) plane.

From this primary analysis of the profiles shown in figure 4 and 5. The results found present correctly the desired profiles, despite the presence of small oscillations. For example, the heat capacity ratio profile a sudden drop in density is created between $x = 0.28$ and $x = 0.32$.

D. RICHTMYER MICHKOV INSTABILITY

Richtmyer-Michkov instability is one of the most interesting tests which have been the subject of several experimental and numerical studies [31, 32, 33, 34]. This instability occurs when an interface separating two fluids of different densities is disturbed by a pulsed shock wave. This instability is produced when an interface separating two fluids of different densities is disturbed by a pulsed shock wave. The shock wave will be the trigger that will provide the necessary impetus to disrupt the interface from its initial state, this leads to an instability known as Richtmyer-Michkov instability. It is a process that is characterized by the development of the interface in three stages, the first is called the linear phase, where the initial amplitude of the disturbance increases linearly with time, followed by a stage called a nonlinear transient stage that allows the appearance of asymmetric bubbles and spikes (characterized by the development of asymmetric "bubbles" and "spikes"). And it ends with a turbulent phase which is the mixing phase. In this article, we will limit ourselves to interfaces of simple geometry with sinusoidal structures.

Take the case of an interaction of a two-dimensional interface with a single principal curvature, the interface is defined by the following equation curve:

$$x_{int} = x_0 - cos(ky), y[0, 1], : x_0 = 1.2$$

$k = 2\pi/\lambda$ is the wave number of perturbations, the

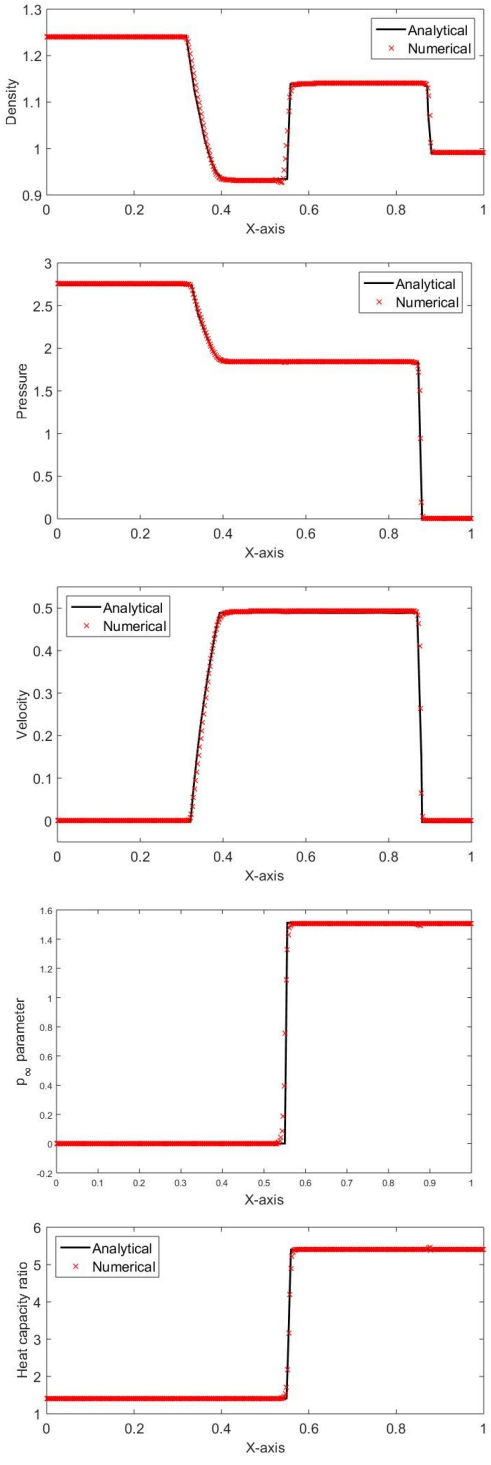

Fig. 3: Comparison of analytical and numerical results using Van Albada limiter for density, pressure, γ and p_∞ parameters and velocity profiles.

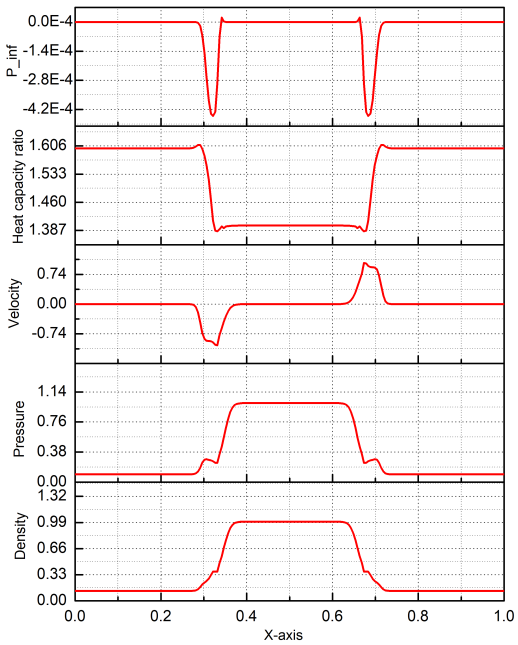

Fig. 4: Results of the shock-tube problem at $t_{final} = 0.025$, for the profiles of density, velocity u, pressure, p_∞ and heat capacity ratio'γ' along the x-axis, with y=0.5 and z=0.5.

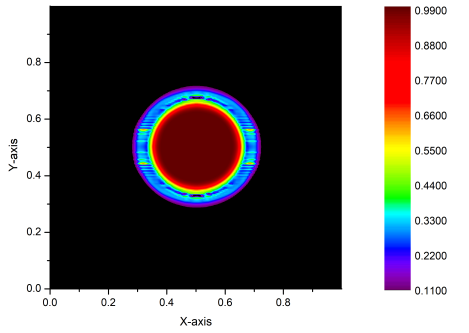

(a) Pressure

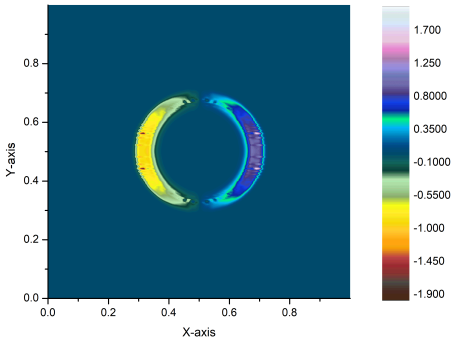

(b) Velocity u

Fig. 5: Pressure (a) and velocity u (b) distributions on the plane z = 0 at t = 0.025

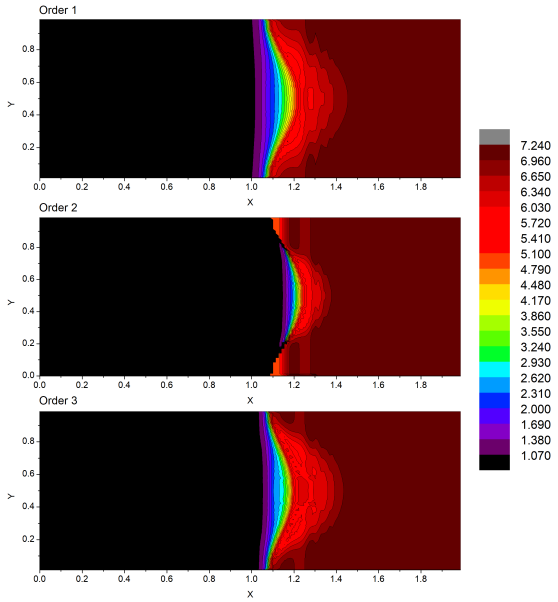

Fig. 6: Richtmayer-Michkov instability for density at $t = 0.1$.

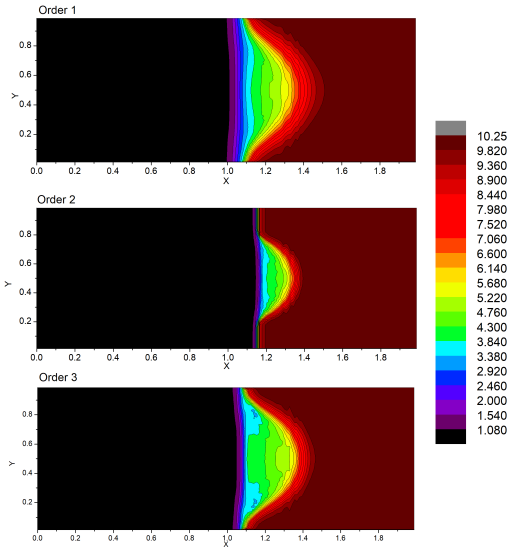

Fig. 7: Richtmayer-Michkov instability for pressure at $t = 0.1$.

wavelength $\lambda = 1$. Regarding the shock wave, it is positioned at $x_s = 1.325$. The state variables inside the tube are divided into three regions:

$$\begin{cases} (\rho, u, p, \gamma, p_\infty)_L = (1.0, 0.0, 1.0, 1.4, 0.0), & x < x_{int} \\ (\rho, u, p, \gamma, p_\infty)_M = (5.0, 0.0, 1.0, 4.0, 1.0), & x_{int} < x < x_s \\ (\rho, u, p, \gamma, p_\infty)_R = (7.093, -0.7288, 10.0, 4.0, 1.0), & x > x_s \end{cases}$$

With v and w are zero everywhere.

We choose a three-dimensional domain $[0, 2] \times [0, 1] \times [0, 1]$ containing $[149 \times 71 \times 5]$ meshes with a time step of $\Delta t = 0.0001$, while using the Van Leer limiter. The choice of order is made by comparing the different results obtained at $t = 0.1$, for the different orders. Figure 6 and 7 show the comparison of density and pressure respectively for the three orders. This is shown in figure 6 for density and figure 7 for pressure.

It can be seen that the results obtained adequately describe the characteristic behavior of fluids. However, the adoption of numerical flow expressions capable of achieving 3rd order precision has yielded the best-desired results [17, 35].

The density and pressure distribution fields at $t = 0.3$ and at $t = 0.5$ are shown in figure 8 and 9 respectively.The interference of pressure waves have caused quite complex flow field as it was also noticed in other references.

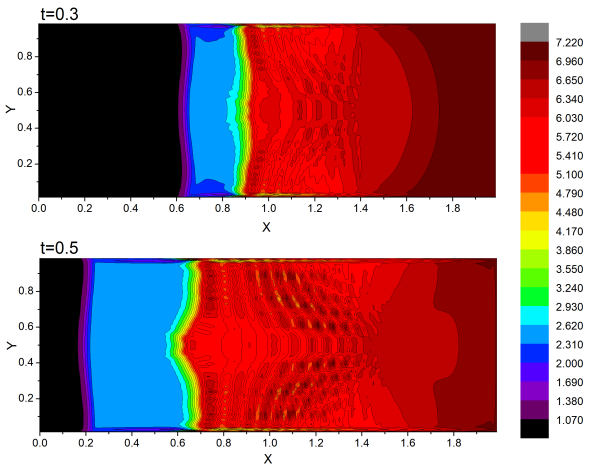

Fig. 8: Richtmayer-Michkov instability for density at t=0.3 and t=0.5.

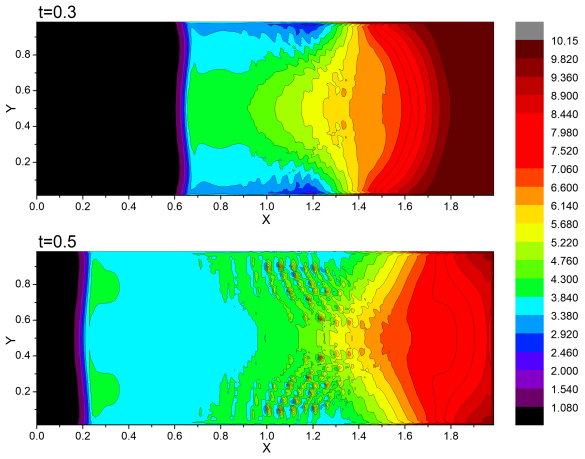

Fig. 9: Richtmayer-Michkov instability for pressure at t=0.3 and t=0.5.

V. Conclusion

The main objective of this paper is to build a numerical algorithm capable of describing shocks and discontinuities for different types of fluids. Based on the Riemann Roe type solver, the numerical algorithm we have developed applies to a wide range of multi-species flows. The MUSCL procedure was combined with the two chosen slope limiters, Van Leer and Van Albada, to increase the order of accuracy in space. This combination allowed the development of an accurate, flexible, and robust method. The results obtained are auspicious as they show similarity with those obtained in the literature at a scale up to three dimensions with a less time-consuming method, especially for multi-species flows. The next objective is to develop the method for application to viscous ids.

References

[1] Toro, Eleuterio F. "The generalized Riemann problem." Riemann Solvers and Numerical Methods for Fluid Dynamics. Springer, Berlin, Heidelberg, 2009. 625-653.

[2] LeVeque, Randall J. Finite volume methods for hyperbolic problems. Vol. 31. Cambridge university press, 2002.

[3] Godunov, Sergei, and I. Bohachevsky. "Finite difference method for numerical computation of discontinuous solutions of the equations of fluid dynamics." Matematičeskij sbornik 47.3 (1959): 271-306.

[4] Toro, Eleuterio F. "The Riemann problem: solvers and numerical fluxes." Handbook of Numerical Analysis. Vol. 17. Elsevier, 2016. 19-54.

[5] Engquist, Björn, and Stanley Osher. "Stable and entropy satisfying approximations for transonic flow calculations." Mathematics of Computation 34.149 (1980): 45-75.

[6] Roe, Philip L. "Approximate Riemann solvers, parameter vectors, and difference schemes." Journal of computational physics 43.2 (1981): 357-372.

[7] Roe, Ph L. "The use of the Riemann problem in finite difference schemes." Seventh International Conference on Numerical Methods in Fluid Dynamics. Springer, Berlin, Heidelberg, 1989.

[8] Quirk, James J. "A contribution to the great Riemann solver debate." Upwind and High-Resolution Schemes. Springer, Berlin, Heidelberg, 1997. 550-569.

[9] Toro, E. F., and V. A. Titarev. "ADER schemes for scalar non-linear hyperbolic conservation laws with source terms in three-space dimensions." Journal of Computational Physics 202.1 (2005): 196-215.

[10] van Leer, Bram. "An introduction to the article "Reminiscences about difference schemes" by SK Godunov." Journal of Computational Physics 153.1 (1999): 1-5.

[11] Harten, Ami, et al. "Uniformly high order accurate essentially non-oscillatory schemes, III." Upwind and high-resolution schemes. Springer, Berlin, Heidelberg, 1987. 218-290.

[12] Jiang, Guang-Shan, and Chi-Wang Shu. "Efficient implementation of weighted ENO schemes." Journal of computational physics 126.1 (1996): 202-228.

[13] Hu, Changqing, and Chi-Wang Shu. "Weighted essentially non-oscillatory schemes on triangular meshes." Journal of Computational Physics 150.1 (1999): 97-127.

[14] Toro, Eleuterio F., R. C. Millington, and L. A. M. Nejad. "Towards very high order Godunov schemes." Godunov methods. Springer, New York, NY, 2001. 907-940.

[15] Titarev, Vladimir A., and Eleuterio F. Toro. "ADER: Arbitrary high order Godunov approach." Journal of Scientific Computing 17.1 (2002): 609-618.

[16] Deng, Xi, et al. "High resolution multi-moment finite volume method for supersonic combustion on unstructured grids." Applied Mathematical Modelling 66 (2019): 404-423.

[17] Shyue, Keh-Ming. "An efficient shock-capturing algorithm for compressible multicomponent problems." Journal of Computational Physics 142.1 (1998): 208-242.

[18] Janan, M. Taha, and A. El Marjani. "A flow solver for the Euler and Navier-Stokes equations for multiphase flows with a stiffened gas equation of state." International Journal of Numerical Methods for Heat Fluid Flow (2007).

[19] Cocchi, J. P., R. Saurel, and J. C. Loraud. "Treatment of interface problems with Godunov-type schemes." Shock waves 5.6 (1996): 347-357.

[20] Saurel, Richard, and Rémi Abgrall. "A simple method for compressible multifluid flows." SIAM Journal on Scientific Computing 21.3 (1999): 1115-1145.

[21] Saurel, Richard, and Rémi Abgrall. "A multiphase Godunov method for compressible multifluid and multiphase flows." Journal of Computational Physics 150.2 (1999): 425-467.

[22] Toro, Eleuterio F. "FORCE Fluxes in Multiple

Space Dimensions." Riemann Solvers and Numerical Methods for Fluid Dynamics. Springer, Berlin, Heidelberg, 2009. 597-623.
[23] Roe, P. L. "Upwind schemes using various formulations of the Euler equations." Numerical Methods for the Euler equations of fluid dynamics 21 (1985): 14.
[24] Osher, Stanley, and James A. Sethian. "Fronts propagating with curvature-dependent speed: Algorithms based on Hamilton-Jacobi formulations." Journal of computational physics 79.1 (1988): 12-49.
[25] Peng, Jun, et al. "An adaptive characteristic-wise reconstruction WENO-Z scheme for gas dynamic Euler equations." Computers Fluids 179 (2019): 34-51.
[26] Benakrach, H., M. Taha-Janan, and M. Z. Es-Sadek. "Simulation of compressible and incompressible flows in the presence of shocks." MATEC Web of Conferences. Vol. 286. EDP Sciences, 2019.
[27] Sod, Gary A. "A survey of several finite difference methods for systems of nonlinear hyperbolic conservation laws." Journal of computational physics 27.1 (1978): 1-31.
[28] Ferrer, Pedro José Martínez, et al. "A detailed verification procedure for compressible reactive multicomponent Navier–Stokes solvers." Computers Fluids 89 (2014): 88-110.
[29] Cocchi, Jean-Pierre, and Richard Saurel. "A Riemann problem based method for the resolution of compressible multimaterial flows." Journal of Computational Physics 137.2 (1997): 265-298.
[30] Niu, Yang-Yao. "Advection upwinding splitting method to solve a compressible two-fluid model." International journal for numerical methods in fluids 36.3 (2001): 351-371.
[31] Luo, Xisheng, et al. "Principal curvature effects on the early evolution of three-dimensional single-mode Richtmyer-Meshkov instabilities." Physical Review E 93.2 (2016): 023110.
[32] Luo, Xisheng, et al. "Richtmyer-Meshkov instability of a three-dimensional SF 6-air interface with a minimum-surface feature." Physical Review E 93.1 (2016): 013101.
[33] Luo, Xisheng, Xiansheng Wang, and Ting Si. "The Richtmyer–Meshkov instability of a three-dimensional air/SF6 interface with a minimum-surface feature." Journal of Fluid Mechanics 722 (2013).
[34] Tritschler, V. K., et al. "Numerical simulation of a Richtmyer–Meshkov instability with an adaptive central-upwind sixth-order WENO scheme." Physica Scripta 2013.T155 (2013): 014016.
[35] Taha-Janan, M. "Contribution à la simulation numérique d'écoulements multi-espèces pour des fluides compressibles ou faiblement compressibles." Thèse de doctorat Es-Sciences appliquées, Université Mohamed V, Ecole Mohammadia d'Ingénieurs (2001).

First A. Author (M'76–SM'81–F'87) and the other authors may include biographies at the end of regular papers. Biographies are often not included in conference-related papers. This author became a Member (M) of NAUN in 1976, a Senior Member (SM) in 1981, and a Fellow (F) in 1987. The first paragraph may contain a place and/or date of birth (list place, then date). Next, the author's educational background is listed. The degrees should be listed with type of degree in what field, which institution, city, state or country, and year degree was earned. The author's major field of study should be lower-cased.

The second paragraph uses the pronoun of the person (he or she) and not the author's last name. It lists military and work experience, including summer and fellowship jobs. Job titles are capitalized. The current job must have a location; previous positions may be listed without one. Information concerning previous publications may be included. Try not to list more than three books or published articles. The format for listing publishers of a book within the biography is: title of book (city, state: publisher name, year) similar to a reference. Current and previous research interests ends the paragraph.

The third paragraph begins with the author's title and last name (e.g., Dr. Smith, Prof. Jones, Mr. Kajor, Ms. Hunter). List any memberships in professional societies other than the NAUN. Finally, list any awards and work for NAUN committees and publications. If a photograph is provided, the biography will be indented around it. The photograph is placed at the top left of the biography. Personal hobbies will be deleted from the biography

Contribution of individual authors to the creation of a scientific article (ghostwriting policy)

Author Contributions: Please, indicate the role and the contribution of each author:

Example

Chen Lee carried out the simulation and the optimization.

Kemal Mehmet has implemented the Algorithm 3.2 and 15.1 in Java

George Luton has organized and executed the experiments of Section 4.

Michael Walton was responsible for the Simulation and Statistics.

In general, please, follow
http://naun.org/main/format/contributor-role.pdf

Sources of funding for research presented in a scientific article or scientific article itself

Report potential sources of funding if there is any